

Synthesis of $H_xLi_{1-x}LaTiO_4$ from Quantitative Solid State Reactions at Room Temperature

Thomas W. S. Yip, Edmund J. Cussen^{*} and Donald MacLaren

Supplementary Information

Experimental Methods

The sodium precursor was prepared by conventional ceramic methods: 40 mol% excess of sodium carbonate and stoichiometric quantities of dried lanthanum oxide and titanium(III) oxide were intimately ground for 30 min, pressed into pellets, heated in air from room temperature to 800 °C at 1 °C min⁻¹ in an open alumina crucible, and held at this temperature for 12 hr; the pellets were cooled to room temperature over several hours. The sample was then ground with a further 40 mol% excess of sodium carbonate, repelleted, subjected to a second heating from 700 °C to 950 °C at 2.5 °C min⁻¹, and held at this temperature for 24 hr. Unreacted sodium carbonate was removed by washing the ground product with 200 ml of distilled water. The washed sample was then dried in air for 1 hour at 120 °C to give a sample of NaLaTiO₄ that X-ray diffraction showed was free from impurities.

HLaTiO₄ was prepared by suspending NaLaTiO₄ (6.502 g) in deuterated nitric acid (~ 475 ml), which was diluted to a concentration of ~ 0.1 mol dm⁻³ (D⁺ in 2-fold excess) with D₂O. This suspension was stirred at room temperature for ca. 2 days in N₂ atmosphere. The exchanged product was then filtered under vacuum and washed with ~ 200 ml of D₂O before being dried at 120 °C for ca. 1 hr in air.

The compounds H_{1-x}Li_xLaTiO₄ (x = 0.1, 0.25, 0.5, 0.75, 0.9 and 1.0) was prepared by grinding stoichiometric quantities of lithium hydroxide monohydrate with up to 4 g of HLaTiO₄ under ambient conditions using an agate mortar and pestle for a total of 30 min. As the two reagents were intimately ground the mixture became less friable but did not develop into a paste. This mixture was then left at room temperature for ca. 2 days in air to give a product that X-ray powder diffraction measurements identified as a single-phase. In order to produce sufficient quantities of material for neutron powder diffraction measurements and also to maximize the degree of sample homogeneity, a sample of HLaTiO₄ was divided into a maximum of 5 portions and each ground with stoichiometric amounts of LiOH·H₂O for 15 min before being combined together and ground for a further 15 min.

X-ray powder diffraction data were collected from samples contained in an aluminium sample holder using a Siemens D500 diffractometer operating with Cu K α radiation in Bragg Brentano geometry. Data were collected at room temperature over the range 10 ≤ 2θ/° ≤ 80 using a step size of Δ2θ = 0.02°.

Neutron diffraction experiments were carried out on the H_{0.5}Li_{0.5}LaTiO₄ composition in order to directly probe the proton and lithium content of this phase. Neutron powder

diffraction experiments were performed using the constant wavelength diffractometer D2B at the Institut Laue Langevin. Data were collected over the angular range $10 \leq 2\theta/\text{°} \leq 155$ at wavelengths of 1.54 and 2.40 Å. The structure of $\text{H}_{0.5}\text{Li}_{0.5}\text{LaTiO}_4$ was refined simultaneously against both of these data sets using the Rietveld method,¹ as implemented in the GSAS suite of programs,² using pseudo-Voigt and shifted Chebyshev functions to describe the peak shape and background, respectively. These data were fitted in the space group P4/nmm using the structure of HLaTiO₄ as a starting point for the Rietveld refinement. This identified a mixture of protons and lithium in the interlayer galleries between the TiO₆ layers. The H/Li content was refined freely within the constraints of charge balance in the structure and this analysis identified a composition $\text{H}_{0.46(2)}\text{Li}_{0.54(2)}\text{LaTiO}_4$ that gave excellent agreement with the target stoichiometry. Attempts to refine the positional coordinates of the proton led to an unstable refinement due to the extremely low occupancy of the site. Consequently, the proton positions were fixed at the coordinates derived for the x=0 member of the series, HLaTiO₄, where the higher proton site occupancy permitted refinement of this position. The final refinement of the data collected from $\text{H}_{0.5}\text{Li}_{0.5}\text{LaTiO}_4$ constrained the composition to that of the reaction mixture to give the structural model listed in Table S1.

Scanning electron micrographs were collected using an FEI Sirion 200 scanning electron microscope from samples loaded onto conductive carbon pads.

Transmission electron microscopy (TEM) was conducted on an FEI Tecnai F20 transmission electron microscope operating at 200 kV and equipped with a field emission gun. Specimens were ground by mortar and pestle and the resultant powder was dispersed in isopropyl alcohol and spotted onto a holey carbon film supported by a copper grid.

The temperature stability of these materials was evaluated using a Perkin Elmer TGA 7 thermal gravimetric analyser. Samples contained in platinum pans were equilibrated at 38 °C and then heated to 50 °C then held isothermally for 5 mins before being heated to 500 °C at a rate of 10 °C min⁻¹. The experiments were conducted under a dynamic atmosphere of dry helium. The rate of mass loss was linear at low (~ 120 °C) and high (> 600 °C) temperatures. The mass loss due to dehydration was taken between limits defined by the departure from linearity in these regions. These observations are similar to those in the literature for the HLaTiO₄ end member of the series.[18] A representative plot of mass loss is shown in Figure S4.

A sample of $\text{H}_{0.5}\text{Li}_{0.5}\text{LaTiO}_4$ (~ 0.6 g) was pressed into a pellet under a load of 2 tonnes and painted with platinum electrodes ~ 5 mm in diameter. This was sintered at 600 °C for 4 hr to yield a pellet of dimensions 9.97 mm in diameter and 2.17 mm in thickness. Conductivity measurements were performed in air using a two-probe cell on heating between 320 °C and 560 °C in 40 °C steps. At each temperature the sample was thermally equilibrated for ≥ 1 hr. Conductivity data were collected using a Solartron 1260 frequency response analyser in the frequency range 1 MHz to 200 mHz using an ac voltage of 100 mV (rms). The experimental data were fitted using the ZView program using an equivalent circuit composed of a resistor and constant phase element in parallel connected in series to another resistor and constant phase element connected in parallel.³ The total resistance was taken as the sum of the two resistances.

1. H. M. Rietveld, *Acta Cryst.*, 1969, **2**, 65.
2. A. C. Larson and R. B. von Dreele, *General Structure Analysis System (GSAS)*, Los Alamos National Laboratories, 1990.
3. F. Le Berre, M.-P. Crosnier-Lopez, Y. Laligant, E. Suard, O. Bohnke, J. Emery and J.-L. Fourquet, *Journal of Materials Chemistry*, 2004, **14**, 3558.

Table S1 Atomic parameters for $H_{0.5}Li_{0.5}LaTiO_4$ derived from neutron diffraction data collected at room temperature.

Atom	Site	Occ.	x	y	z	$100U_{iso} / \text{\AA}^2$
La	2c	1	$\frac{1}{4}$	$\frac{1}{4}$	0.8814(2)	1.23(6)
Ti	2c	1	$\frac{1}{4}$	$\frac{1}{4}$	0.2966(4)	1.09(13)
O1	4f	1	$\frac{3}{4}$	$\frac{1}{4}$	0.7445(2)	0.94(5)
O2	2c	1	$\frac{1}{4}$	$\frac{1}{4}$	0.4401(3)	1.74(9)
O3	2c	1	$\frac{1}{4}$	$\frac{1}{4}$	0.0795(2)	1.12(8)
Li	2a	0.5	$\frac{1}{4}$	$\frac{3}{4}$	$\frac{1}{2}$	2.2(4)
H	16k	0.063	0.387	0.068	0.4869	2.89(13)

P4/nmm: $a = 3.75083(14) \text{ \AA}$, $c = 12.2160(7) \text{ \AA}$, Vol. = $171.86(2) \text{ \AA}^3$

$R_{wp} = 4.48$ | $R_p = 3.45$ | $\chi^2 = 3.789$ for 40 variables

Supplementary Information Figure Captions

Figure S1 Scanning electron microscopy images collected from (a) and (b) NaLaTiO₄, (c) and (d) HLaTiO₄ and (e) and (f) H_{0.5}Li_{0.5}LaTiO₄.

Figure S2 The neutron powder diffraction profile collected from H_{0.5}Li_{0.5}LaTiO₄ at room temperature at a wavelength, $\lambda = 2.40 \text{ \AA}$. The observed data are shown as dots and the calculated pattern is shown as a solid line. Allowed Bragg peaks are indicated by vertical bars.

Figure S3 (a,b) Transmission electron microscopy image of two grains and (c,d) associated high resolution images collected from the indicated regions, with (inset) Fourier transforms of the images. Lattice fringes are evident in both areas and give rise to strongly peaked, slightly streaked Fourier transforms, indicating long-range crystallinity. Grains generally comprise of several crystallites and had a laminar appearance such as that of (c), however the observation of sharp peaks, rather than rings, in both Fourier transforms and electron diffraction patterns (not shown) indicates crystallographic registry between laminar crystallites.

Figure S4 Thermal gravimetric data showing the variation in mass as a function of temperature for sample H_{0.5}Li_{0.5}LaTiO₄ heated from 38 °C to 800 °C under a dynamic atmosphere of dry helium. The sample was heated at a rate of 10 °C min⁻¹ to 120 °C and held at this temperature for 1 hr before being heated to 800 °C at 10 °C min⁻¹.

Figure S5 The mass loss observed on heating H_{1-x}Li_xLaTiO₄ represented as the number of molecules of water per formula unit. Multiple circles for a single composition indicate experiments repeated using samples prepared from repeated syntheses. The quantity of water anticipated to be produced by reaction Equation [2] is indicated by a line.

Figure S6 X-ray powder diffraction data collected from a sample of H_{0.5}Li_{0.5}LaTiO₄ that has been dehydrated by heating to 480°C to give a nominal stoichiometry of Li_{0.5}LaTiO_{3.75}. The pattern can be indexed using a tetragonal cell (P4/nmm; $a = 3.775(2)$, $c = 11.852(10)$ Å) as shown by the vertical markers. The Miller indices are shown for selected reflections.

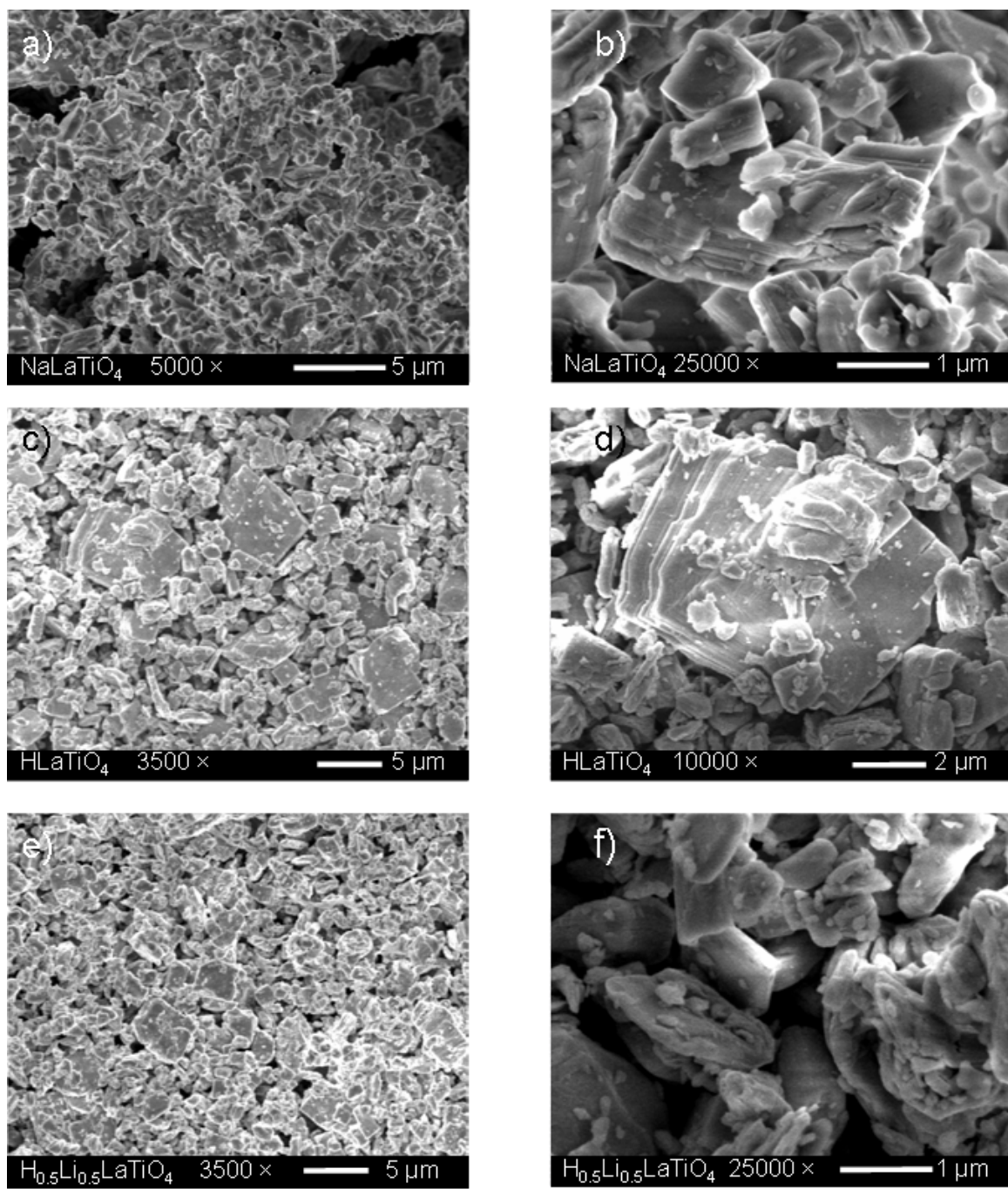


Figure S1 Scanning electron microscopy images collected from (a) and (b) NaLaTiO_4 , (c) and (d) HLaTiO_4 and (e) and (f) $\text{H}_{0.5}\text{Li}_{0.5}\text{LaTiO}_4$.

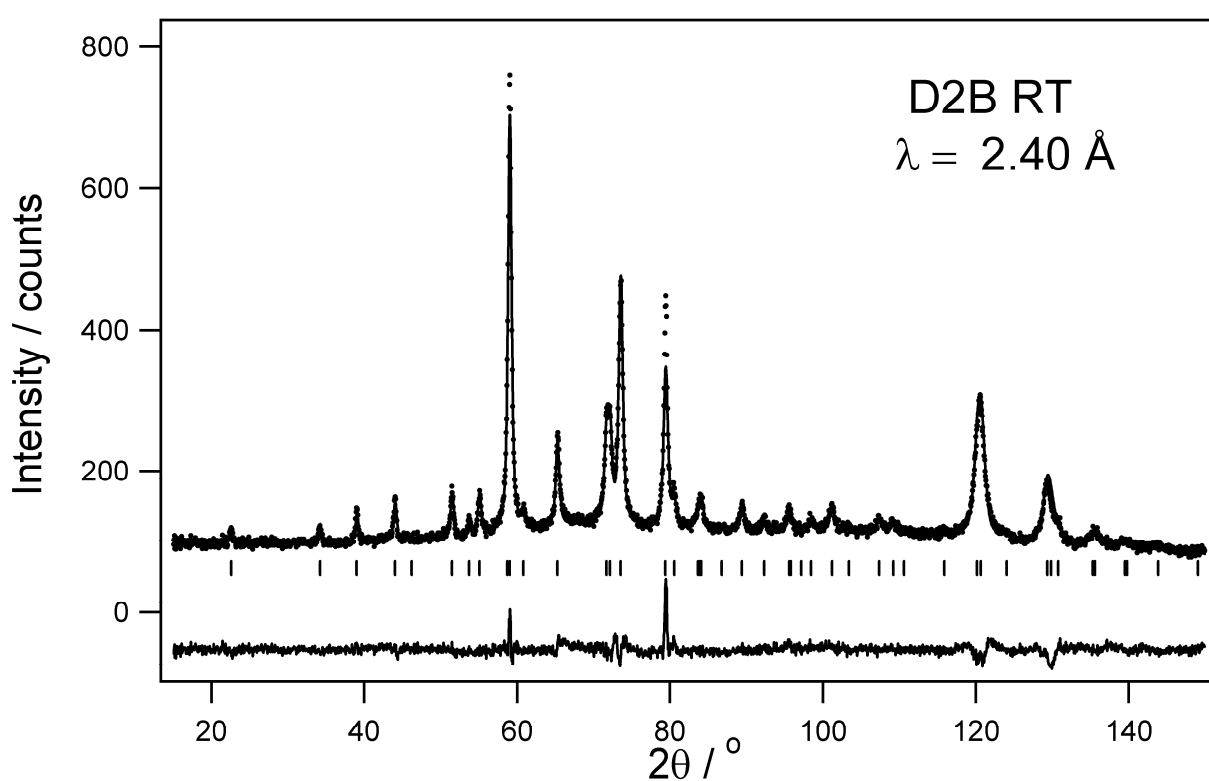


Figure S2 The neutron powder diffraction profile collected from $\text{H}_{0.5}\text{Li}_{0.5}\text{LaTiO}_4$ at room temperature at a wavelength, $\lambda = 2.40 \text{ \AA}$. The observed data are shown as dots and the calculated pattern is shown as a solid line. Allowed Bragg peaks are indicated by vertical bars.

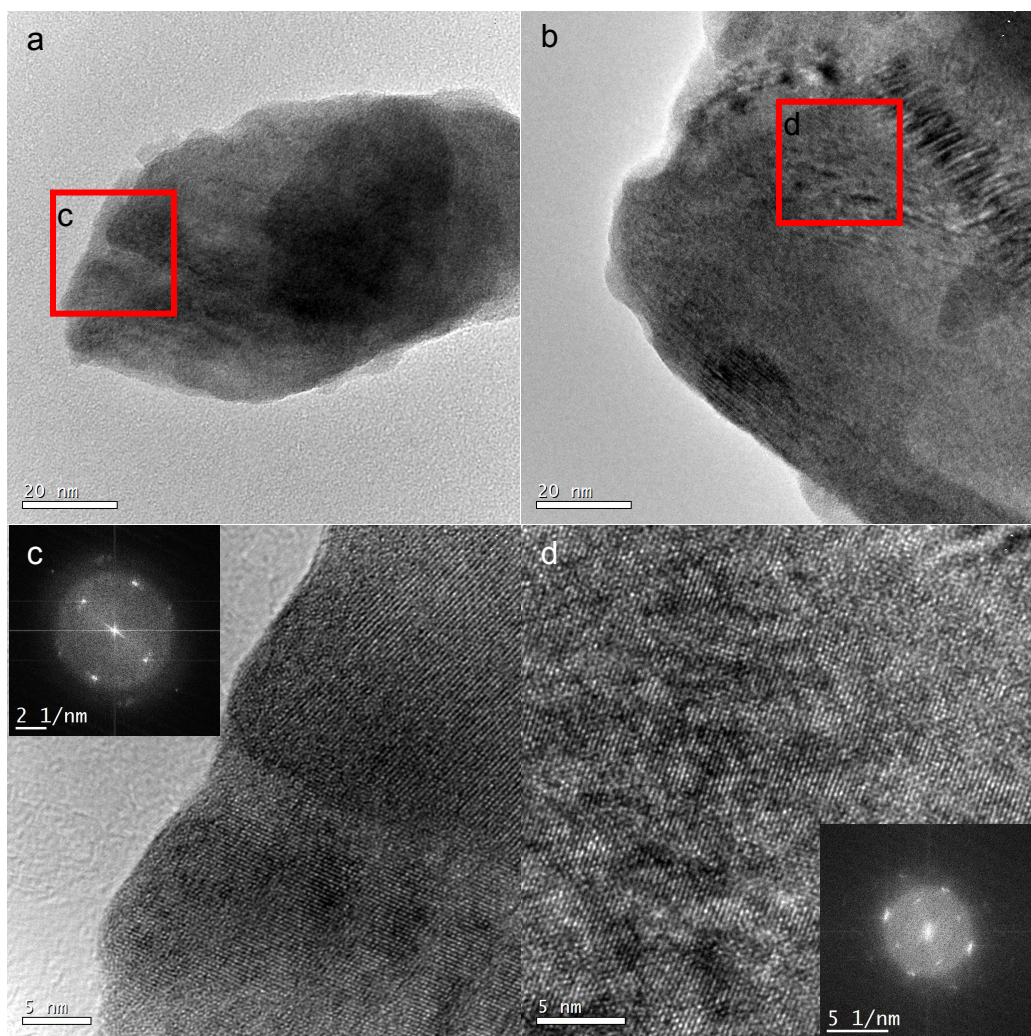


Figure S3 (a,b) Transmission electron microscopy image of two grains and (c,d) associated high resolution images collected from the indicated regions, with (inset) Fourier transforms of the images. Lattice fringes are evident in both areas and give rise to strongly peaked, slightly streaked Fourier transforms, indicating long-range crystallinity. Grains generally comprise of several crystallites and had a laminar appearance such as that of (c), however the observation of sharp peaks, rather than rings, in both Fourier transforms and electron diffraction patterns (not shown) indicates crystallographic registry between laminar crystallites.

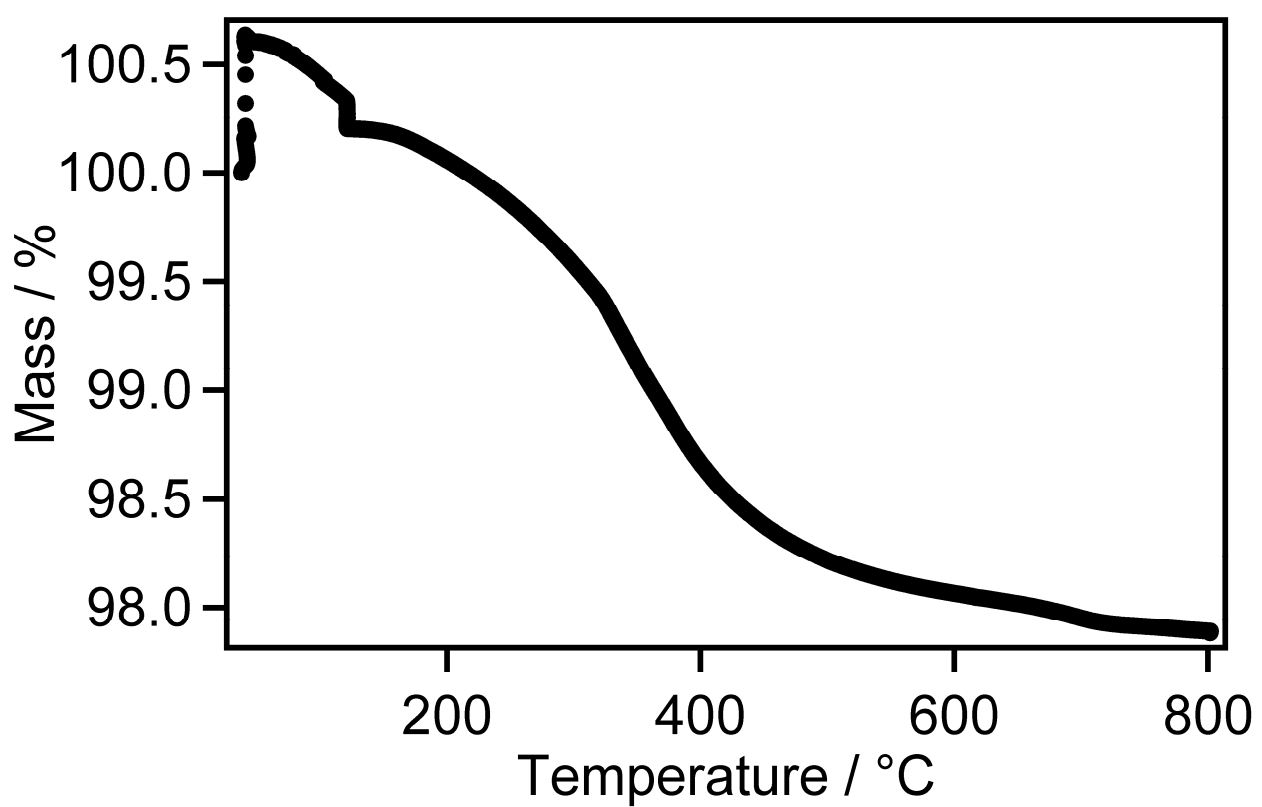


Figure S4 Thermal gravimetric data showing the variation in mass as a function of temperature for sample $\text{H}_{0.5}\text{Li}_{0.5}\text{LaTiO}_4$ heated from 38 °C to 800 °C under a dynamic atmosphere of dry helium. The sample was heated at a rate of 10 °C min⁻¹ to 120 °C and held at this temperature for 1 hr before being heated to 800 °C at 10 °C min⁻¹.

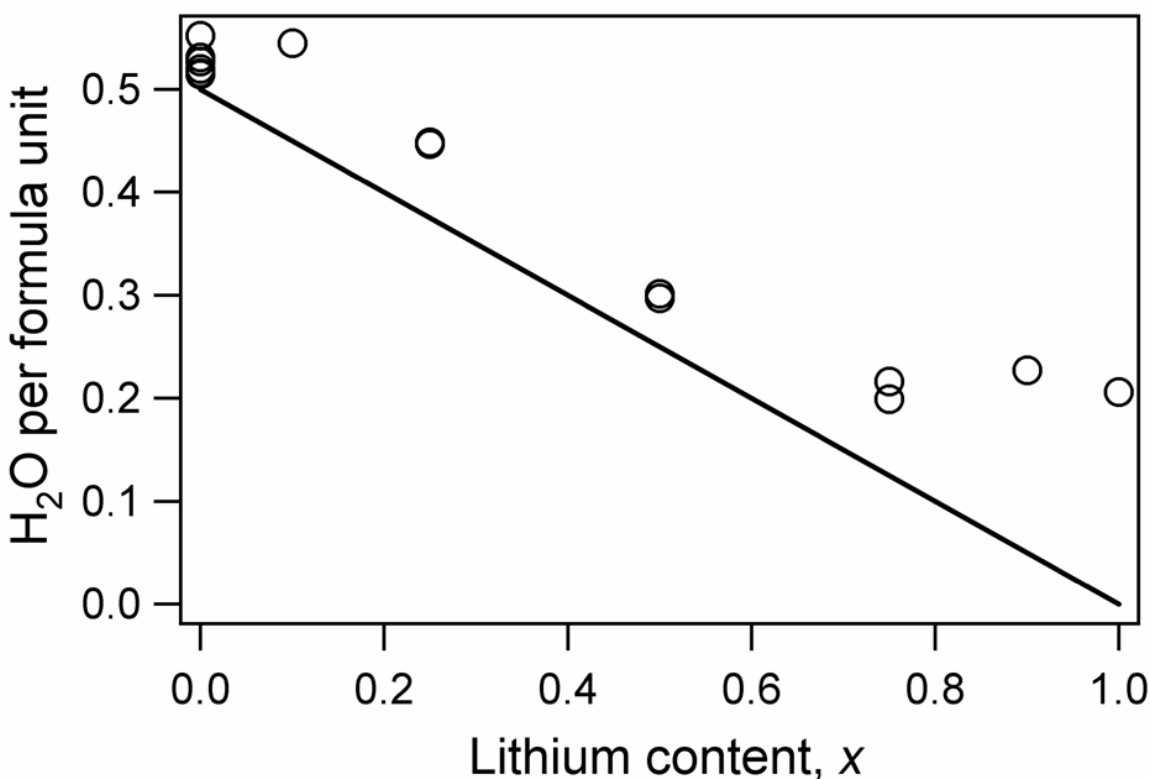


Figure S5 The mass loss observed on heating $H_{1-x}Li_xLaTiO_4$ represented as the number of molecules of water per formula unit. Multiple circles for a single composition indicate experiments repeated using samples prepared from repeated syntheses. The quantity of water anticipated to be produced by reaction Equation [2] is indicated by a line.

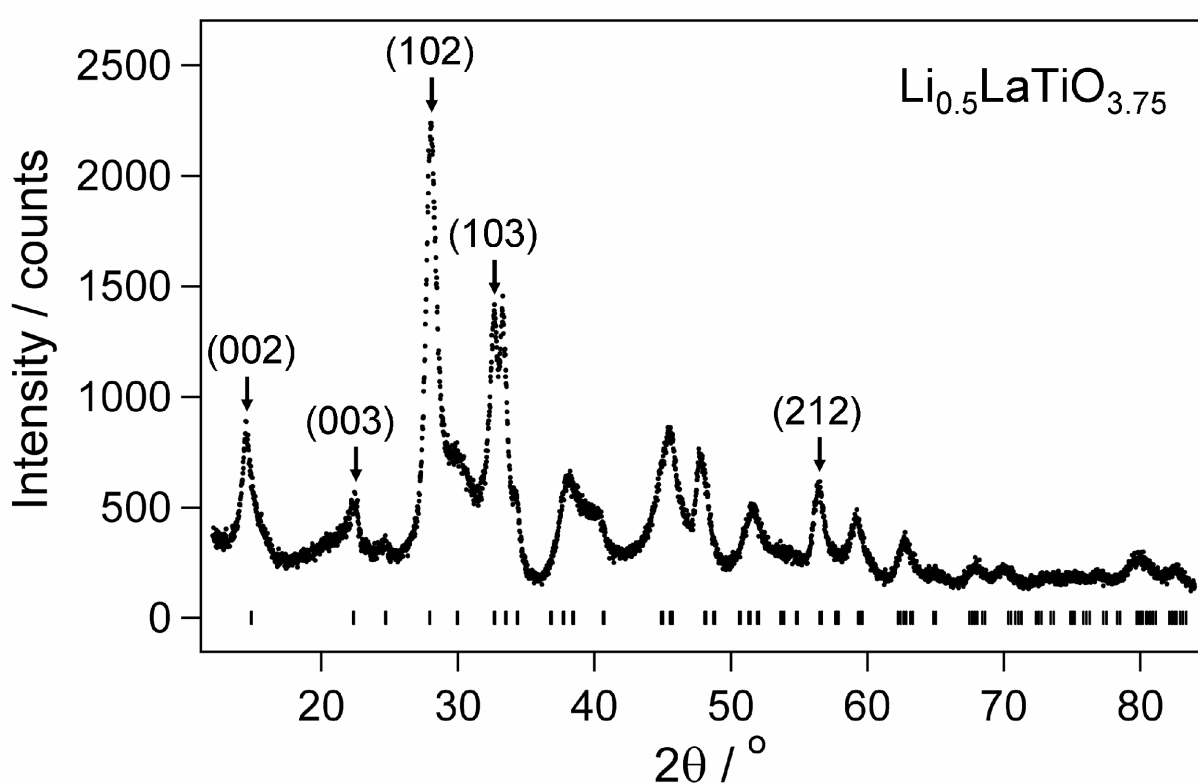


Figure S6 X-ray powder diffraction data collected from a sample of $\text{H}_{0.5}\text{Li}_{0.5}\text{LaTiO}_4$ that has been dehydrated by heating to 480°C to give a nominal stoichiometry of $\text{Li}_{0.5}\text{LaTiO}_{3.75}$. The pattern can be indexed using a tetragonal cell as shown by the vertical markers. The Miller indices are shown for selected reflections.